Vol.2, No.1, 18-25 (2010)
http://dx.doi.org/10.4236/ns.2010.21003

Natural Science

# Hydriding and dehydriding kinetics of melt spun nanocrystalline $Mg_{20}Ni_{10-x}Cu_x$ (x = 0-4) alloys

**Yang-Huan Zhang[1,2,*], Dong-Liang Zhao[1], Bao-Wei Li[2], Hui-Ping Ren[1], Shi-Hai Guo[1], Xin-Lin Wang[1]**

[1]Department of Functional Material Research, Central Iron and Steel Research Institute, Beijing, China
[2]School of Material, Inner Mongolia University of Science and Technology, Baotou, China; zyh59@yahoo.com.cn

Received 22 October 2009; revised 13 November 2009; accepted 17 November 2009.

## ABSTRACT

**The nanocrystalline $Mg_2Ni$-type electrode alloys with nominal compositions of $Mg_{20}Ni_{10-x}Cu_x$ (x = 0, 1, 2, 3, 4) were synthesized by melt-spinning technique. The microstructures of the alloys were characterized by XRD, SEM and HRTEM. The hydrogen absorption and desorption kinetics of the alloys were measured using an automatically controlled Sieverts apparatus. The results show that all the as-spun alloys hold typical nanocrystalline structure. The substitution of Cu for Ni does not change the major phase $Mg_2Ni$ but it leads to the formation of the secondary phase $Mg_2Cu$. The hydrogen absorption capacity of the alloys first increases and then decreases with rising Cu content, but the hydrogen desorption capacity of the alloys monotonously grows with increasing Cu content. The melt spinning significantly improves the hydrogenation and dehydrogenation capacities and kinetics of the alloys.**

**Keywords:** $Mg_2Ni$-Type Alloy; Substituting Ni with Cu; Melt Spinning; Hydriding and Dehydriding Kinetics

## 1. INTRODUCTION

Mg and Mg-based alloys has been considered as potential materials for solid state hydrogen storage in the form of metallic hydrides such as $MgH_2$ and $Mg_2NiH_4$. The theoretical hydrogen storage capacities of $MgH_2$ and $Mg_2NiH_4$ are 7.6 wt.% and 3.6 wt.% [1,2] respectively, which is quite adequate for commercial applications as a hydrogen fuel source [3]. Unfortunately, the slow sorption/desorption kinetics and high dissociation temperature of these kinds of metal hydrides limit their practical application. Therefore, finding ways of improving the hydration kinetics of Mg-based alloys has been one of the main challenges faced by researchers in this area. Various attempts, involving mechanical alloying (MA) [4], GPa hydrogen pressure method [5], melt spinning [6], gravity casting [7], polyol reduction [8], hydriding combustion synthesis [9], surface modification [10], alloying with other elements [11,12], adding catalysts [13] etc, have been undertaken to improve the activation and hydriding property.

Gennari *et al.* [14] reported that the nanocrystalline $Mg_2Ni$ synthesized by combined milling-annealing procedure can readily hydrogen absorption during the first cycle and show excellent absorption kinetics at 200℃. Muthukumar *et al.* [15] confirmed that a maximum hydrogen capacity of 3.67 wt.% for the $Mg_2Ni$ alloy prepared by mechanical alloying (MA) could be achieved for an initial absorption temperature of 300 ℃ and supply pressure of 20 bar. Recham *et al.* [16] found that the hydrogen absorption property of ball-milled $MgH_2$ can be enhanced by adding $NbF_5$, and the milled $MgH_2$+ $NbF_5$ composite can desorbs 3 wt.% $H_2$ at 150℃. Dobrovolsky *et al.* [17] synthesized a $MgH_2$ (50 wt.%) + $TiB_2$ (50 wt.%) composite by intensive mechanical milling and found that $TiB_2$ addition decreases the dissociation temperature of the $MgH_2$ hydride by about 50℃.

Indubitably, ball-milling is a very effective method for the preparation of nanocrystalline and amorphous Mg and Mg-based alloys. Particularly, it is suitable to solubilize particular elements into $MgH_2$ or $Mg_2NiH_4$ above the thermodynamic equilibrium limit, which is helpful to destabilize $MgH_2$ or $Mg_2NiH_4$ [18]. However, the milled Mg and Mg-based alloys show very poor hydrogen absorbing and desorbing stability due to the fact that the metastable structures formed by ball milling tended to vanish during multiple hydrogen absorbing and desorbing cycles [19]. Alternatively, melt-spun technique can overcome the above mentioned shortcoming and effective avoiding the significant degradation of hydrogen absorbing and desorbing cycle properties of Mg and Mg-based [20]. Additionally, the melt-spinning technique is a very effective method to obtain a nanocrystalline structure and is very suitable for mass-production of nanocrystalline Mg-based alloys. It was also clarified that nanocrystalline alloys produced by melt-spinning could

 

have excellent hydriding characteristics even at room temperature, similar to the alloys produced by the MA process. Spassov *et al.* [21] prepared $Mg_2(Ni, Y)$ hydrogen storage alloy with exact composition $Mg_{63}Ni_{30}Y_7$ by rapid solidification, and its maximum hydrogen absorption capacity (about 3.0 wt.%) and hydrogenation kinetics of the as-spun $Mg_2(Ni, Y)$ alloy were found to exceed those of the polycrystalline $Mg_2Ni$ alloys prepared by conventional technology and to be comparable to the hydrogen absorption characteristics of ball-milled nanocrystalline $Mg_2Ni$. It was determined that the addition of third element stabilizes the nanostructure of Mg-Ni based alloy, which could be very important for practical H-storage materials.

Our previous work indicated that the substitution of Co for Ni significantly improved the hydriding and dehydriding kinetics of the $Mg_2Ni$-type alloys [22]. Therefore, it is very desirable to investigate the influence of substituting Ni with Cu on the hydriding and dehydriding characteristics of $Mg_2Ni$-type alloys prepared by melt-spinning. The objective of this work is to produce the Mg-Ni-based ternary nanocrystalline alloys by melt spinning and to examine their structures and hydriding and dehydriding kinetics.

## 2. EXPERIMENTAL METHODS

The alloy ingots were prepared using a vacuum induction furnace in a helium atmosphere at a pressure of 0.04 MPa. Part of the as-cast alloys was re-melted and spun by melt-spinning with a rotating copper roller. The spinning rate was approximately expressed by the linear velocity of the copper roller because it is too difficult to measure a real spinning rate i.e. cooling rate of the sample during spinning. The spinning rates used in the experiment were 15, 20, 25 and 30 m/s, respectively. The nominal compositions of the experimental alloys were $Mg_{20}Ni_{10-x}Cu_x$ (x = 0, 1, 2, 3, 4). For convenience, the alloys were denoted with Cu content as $Cu_0$, $Cu_1$, $Cu_2$, $Cu_3$ and $Cu_4$, respectively.

The morphologies of the as-cast alloys were observed by scanning electron microscope (SEM) (Philips QUANTA 400). The phase structures of the as-cast and spun alloys were determined by XRD diffractometer (D/max/2400). The diffraction, with the experimental parameters of 160 mA, 40 kV and 10°/min respectively, was performed with $CuK_{\alpha 1}$ radiation filtered by graphite. The thin film samples of the as-spun alloys were prepared by ion etching for observing the morphology with high resolution transmission electron microscope (HRTEM) (JEM-2100F, operated at 200 kV), and for determining the crystalline state of the samples with electron diffraction (ED).

The hydrogen absorption and desorption kinetics of the alloys were measured by an automatically controlled Sieverts apparatus. The hydrogen absorption was conducted at 1.5 MPa at 200 ℃ and the hydrogen desorption in a vacuum ($1\times10^{-4}$ MPa) at 200 ℃ too.

## 3. RESULTS AND DISCUSSIONS

### 3.1. Microstructure Characteristics

The SEM images of the as-cast alloy are illustrated in **Figure 1**, displaying a typical dendrite structure. The substitution of Cu for Ni does not change the morphology of the alloys but it causes a significant refinement of the grains. The result obtained by energy dispersive spectrometry (EDS) indicates that the major phase of the as-cast alloys is $Mg_2Ni$ phase (denoted as A). Some small massive matters in the alloys containing Cu can clearly be seen in **Figure 1**, which are determined by EDS to be $Mg_2Cu$ phase (denoted as B).

**Figure 2** presents the XRD profiles of the as-cast and spun $Mg_{20}Ni_{10-x}Cu_x$ (x = 0, 1, 2, 3, 4) alloys, showing that the substitution of Cu for Ni does not change the phase structure. All the as-cast and spun alloys display a single phase structure. This seems to be contrary with the result of SEM observation. It is most probably associated with the fact that $Mg_2Ni$ and $Mg_2Cu$ hold completely identical structure and nearly same lattice constants. On the other hand, the amount of the $Mg_2Cu$ phase is very little so that the XRD observation can not detect its presence. Listed in **Table 1** are the lattice parameters, cell volume and full width at half maximum (FWHM) values of the main diffraction peaks of the as-cast and spun (20 m/s) alloys which were calculated by software of Jade 6.0. It can be derived from **Table 1** that the substitution of Cu for Ni causes the FWHM values of the main diffraction peaks of the as-cast and spun alloys significantly increased, and it leads to the lattice parameters and cell volume of the alloys cleverly enlarged, which is attributed to the slightly larger atomic radius of Cu than Ni. It can be seen from **Table 1** that melt spinning causes the FWHM values of the main diffraction peaks of the alloys significantly increased which is doubtless attributed to the refinement of the grains and the stored stress in the grains produced by melt spinning. Based on the FWHM values of the broad diffraction peak (203) in **Figure 2b**, the crystallite size $\langle D_{hkl} \rangle$ (Å) of the as-spun alloy was calculated using Scherrer's equation. The grain sizes of the as-spun alloys are in a range of 2-6 nm, consistent with results reported by Friedlmeier *et al.* [23]. It is very important to notice that $\langle D \rangle$ values were calculated on the same peak having Miller indices (203) due to better possibility of mutual comparison.

**Figure 3** shows HRTEM micrographs and electron diffraction patterns of the as-spun $Cu_1$ and $Cu_3$ alloys, which reveal a nanocrystalline microstructure, with an average crystal size of about 2-5 nm. This result agrees very well with the XRD observation shown in **Figure 2**.

From HRTEM observations there is some evidence that the as-spun alloys are strongly disordered and nanostructured, but they are free of amorphous phase. Spassov *et al.* [21] reported that Mg-based alloys with nanocrystalline microstructures can be obtained by controlling the cooling rates. The crystal defects in the as-spun alloy, stacking faults (denoted as A), twin-grain boundaries (denoted as B), dislocations (denoted as C) and sub-grain boundaries (denoted as D), can clearly be seen in **Figure 4**.

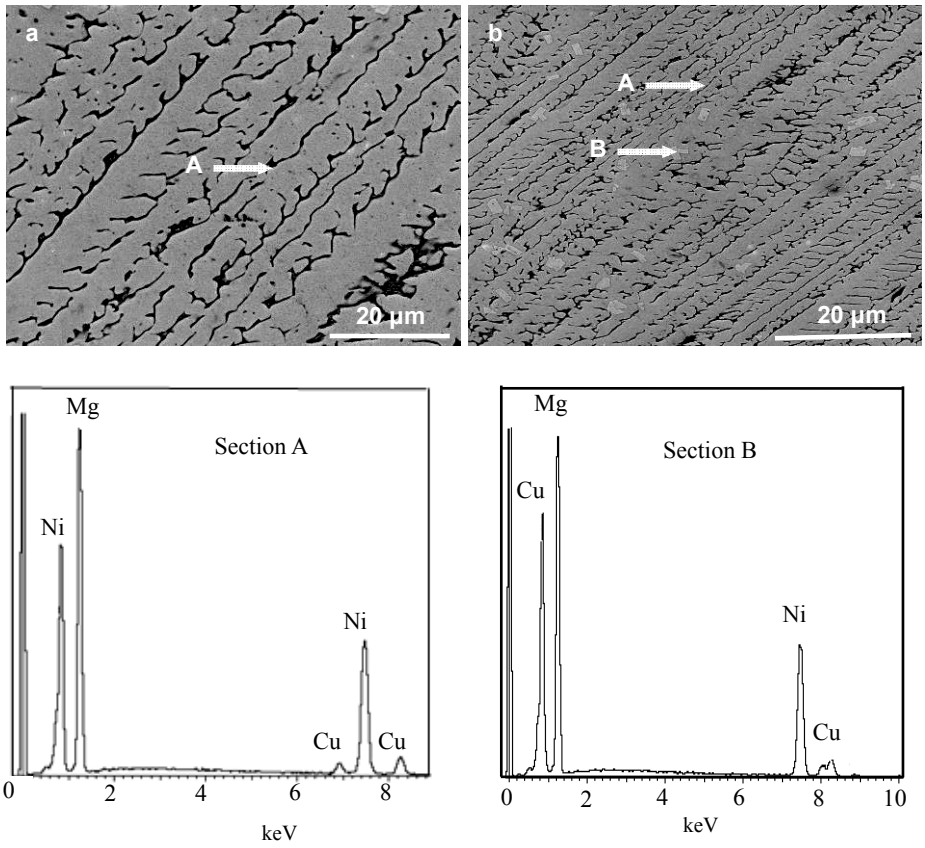


**Figure 1.** SEM images of the as-cast alloys together with EDS spectra of sections A and B in Figure 1 (b): (a) $Cu_0$ alloy, (b) $Cu_4$ alloy.

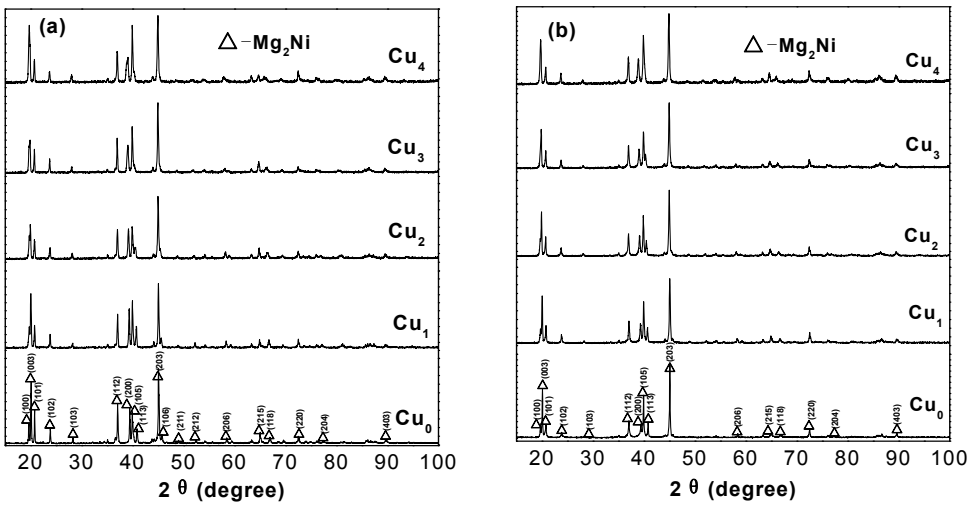


**Figure 2.** XRD profiles of the as-cast and spun alloys: (a) As-cast, (b) As-spun (20 m/s).

 

**Table 1.** The lattice parameters, cell volume and the FWHM values of the major diffraction peaks of the alloys.

| Alloys | FWHM values | | | | Lattice parameters and cell volume | | | | | |
|---|---|---|---|---|---|---|---|---|---|---|
| | 2θ(20.02°) | | 2θ(45.14°) | | a (Å) | | c (Å) | | V (Å$^3$) | |
| | As-cast | 20m/s | As-cast | 20m/s | As-cast | 20 m/s | As-cast | 20 m/s | As-cast | 25 m/s |
| $Cu_0$ | 0.122 | 0.129 | 0.169 | 0.173 | 5.2097 | 5.2101 | 13.244 | 13.258 | 311.29 | 311.67 |
| $Cu_1$ | 0.133 | 0.184 | 0.178 | 0.218 | 5.2102 | 5.2154 | 13.252 | 13.262 | 311.54 | 312.39 |
| $Cu_2$ | 0.148 | 0.232 | 0.183 | 0.223 | 5.2136 | 5.2162 | 13.283 | 13.307 | 312.67 | 313.55 |
| $Cu_3$ | 0.151 | 0.257 | 0.192 | 0.232 | 5.2154 | 5.2171 | 13.297 | 13.313 | 313.22 | 313.80 |
| $Cu_4$ | 0.165 | 0.286 | 0.204 | 0.252 | 5.2171 | 5.2203 | 13.302 | 13.317 | 313.54 | 314.28 |

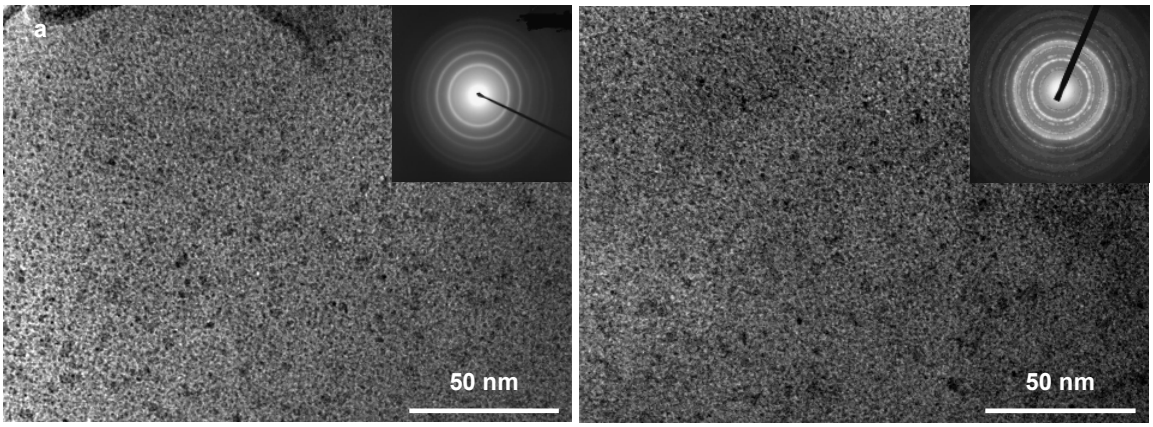


**Figure 3.** HRTEM micrographs and ED of the as-spun alloys (30 m/s): (a) $Cu_1$ alloy (b) $Cu_3$ alloy.

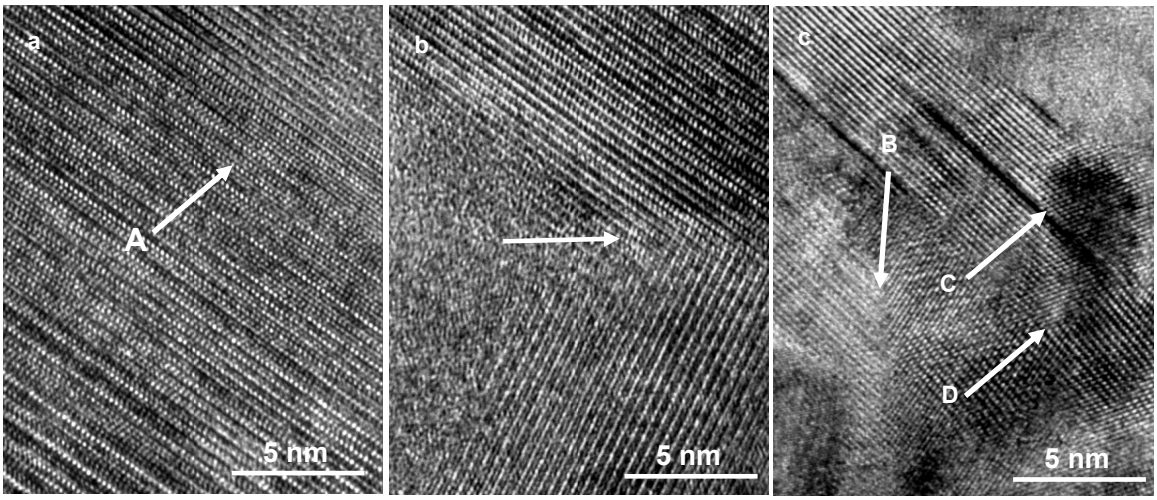


**Figure 4.** Crystal defects in the as-spun (30 m/s) $Cu_3$ alloy taken by HRTEM: (a) Stacking fault, (b) Twin grain boundary, (c) Dislocations and sub-grain boundaries.

## 3.2. Hydriding and Dehydriding Characteristics

**Figure 5** shows the hydrogen absorption capacity and kinetics of the as-cast and spun $Cu_1$ and $Cu_3$ alloys. It can be seen that all the hydriding kinetic curves of the as-spun alloys show an initial fast hydrogen absorption stage after which the hydrogen content is saturated at longer hydrogenation time, indicating that the melt spinning significantly improves the hydrogen absorption property of the alloys. The hydrogen absorption capacities of the alloys increase with rising spinning rate. When the spinning rate grows from 0 (As-cast is defined as spinning rate of 0 m/s) to 30 m/s, the hydrogen absorption capacity of the $Cu_1$ alloy in 10 min rises from 1.99 to 3.12 wt.%, and from 1.74 to 2.88 wt.% for the $Cu_3$ alloy.

The hydrogenation kinetics and storage capacity of all the as-spun nanocrystalline $Mg_2Ni$-type alloys studied

 

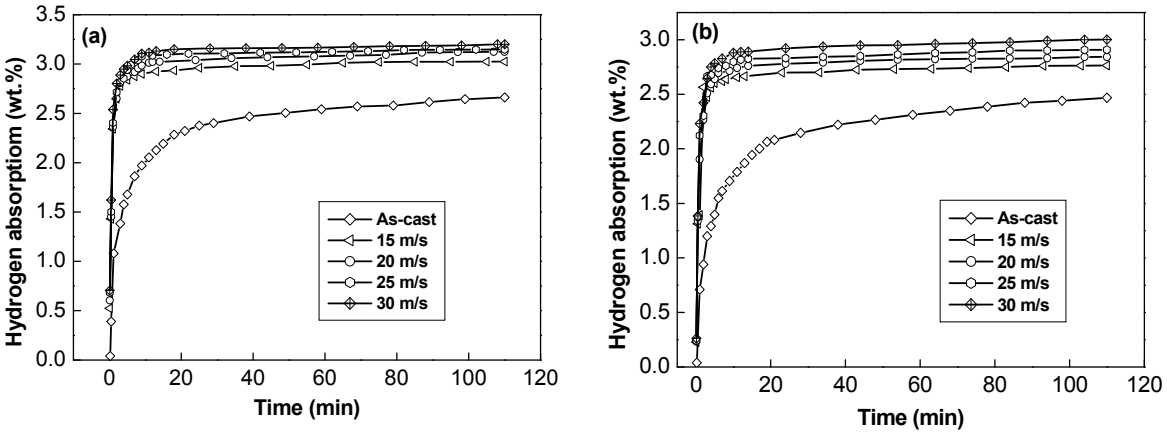


**Figure 5.** Hydrogen absorption kinetic curves of the as-cast and spun alloys: (a) $Cu_1$ alloy (b) $Cu_3$ alloy.

are superior to those of conventional polycrystalline materials with similar composition. The enhanced hydrogenation property by melt spinning is undoubtedly associated with the refinement of the grains produced by melt spinning [24]. By refining the microstructure, a lot of new crystallites and grain boundaries are created which can act as fast diffusion paths for hydrogen absorption. Based on the result reported by Orimo and Fujii [25], the distribution of the maximum hydrogen concentrations in three nanometer-scale regions, i.e. grain region and grain boundary region as well as amorphous region, have been experimentally determined to be 0.3 wt.% H in the grain region of $Mg_2Ni$, 4.0 wt.% H in the grain boundary and 2.2 wt.% H in the amorphous region. It revealed that the hydrides mainly exist in grain-boundary region and the amorphous phase region. The improved hydrogenation characteristics can be explained with the enhanced hydrogen diffusivity in the nanocrystalline microstructure as the nanocrystalline leads to an easier access of hydrogen to the nanograins, avoiding the long-range diffusion of hydrogen through an already formed hydride, which is often the slowest stage of absorption. It is known that the nanocrystalline microstructures can accommodate higher amounts of hydrogen than polycrystalline ones. The crystalline material, when melt spun, becomes at least partially disordered and its structure changes to nanocrystalline. Consequently, high densities of crystal defects such as dislocations, stacking faults and grain boundaries are introduced. The large number of interfaces and grain boundaries available in the nanocrystalline materials provide easy pathways for hydrogen diffusion and accelerates the hydrogen absorbing/desorbing process.

The hydrogen absorption kinetic curves of the as-spun alloys are plotted in **Figure 6**. It can be seen that the hydrogen absorption capacity of as-spun alloys first increases and then decreases with the variation of Cu content. The $Cu_2$ alloy shows a maximum hydrogen absorption capacity at 200℃. The kinetics of hydrogenation was extremely fast so that the alloys absorbed more than 95% of their hydrogen capacities within the first 5 min. The excellent hydriding kinetics is ascribed to the nanocrystalline structure because the high surface to volume ratios (high specific surface area) and the presence of large number of grain boundaries in nanocrystalline alloys enhance the kinetics of hydrogen absorption/ desorption. The positive function of Cu substitution on the hydrogen absorption capacity and kinetics of the alloy is attributed to the increased cell volume and the grain refined by Cu substitution. The increase of the cell volume is very helpful to hydrogen absorption capacity, and the grain boundary possesses the largest hydrogen absorption capability [25]. It was well known that the catalytic action of Ni on hydriding is stronger than Cu. Therefore, it is understandable that a superfluous amount of Cu substitution ($x>2$) must lead to a decrease of the hydrogen absorption capacity of the alloys.

**Figure 7** shows the hydrogen desorption capacity and kinetics of the as-cast and spun $Cu_1$ and $Cu_3$ alloys, indicating that the dehydriding capability of the alloys obviously meliorates with rising spinning rate. When the spinning rate grows from 0 to 30 m/s, the hydrogen desorption capacity of the $Cu_1$ alloy in 20 min increases from 0.29 to 0.98 wt.%, and from 0.52 to 1.49 wt.% for $Cu_3$ alloy, respectively. The nanocrystalline $Mg_2Ni$-based alloys produced by melt spinning exhibit higher H-absorption capacity and faster kinetics of hydriding/ dehydriding than crystalline $Mg_2Ni$. A similar result was reported by Spassov *et al.* [21]. The specific capacity and hydriding/dehydriding kinetics of hydride materials depend on their chemical composition and crystalline structure [26]. The observed essential differences in the hydriding/dehydriding kinetics of the melt-spun nanocrystalline $Mg_2Ni$ type alloys studied most probably have to be associated with the composition of the alloy as well as with the differences in their microstructure due to the different spinning rates. It was reported that

 

the high surface to volume ratios, i.e. high specific surface area, and the presence of large number of grain boundaries in nanocrystalline alloys enhance the kinetics of hydrogen absorption/desorption [21]. Zaluski *et al.* [27] and Orimo *et al.* [28] confirmed that the hydriding/dehydriding characteristics at low temperatures (lower than 200℃) of nanocrystalline $Mg_2Ni$ alloys prepared by mechanical alloying can be improved by reducing the grain size (20-30 nm), due to hydrogen occupation in the disordered interface phase.

The hydrogen desorption kinetic curves of the as-spun alloys are plotted in **Figure 8**. An important feature of the dehydrogenation process in the alloys is very slow initial hydrogen desorption, followed by slack increase in the amount of hydrogen desorbed. **Figure 8** indicates that the Cu substitution significantly improves the hydogen desorption capacity and kinetics of the alloys. When Cu content x increases from 0 to 4, the hydrogen desorption capacity of the as-spun (20 m/s) alloy in 20 min rises from 0.62 to 1.43 wt.%, and from 0.89 to 1.69 wt.% for the as-spun (30 m/s) alloy. Several possibilities can be considered as the reasons why the substitution of Cu for Ni enhances the hydrogen desorption kinetics of $Mg_2Ni$-type alloys. Firstly, the partial substitution of element Cu for Ni in $Mg_2Ni$ compound decreases the stability of the hydride and makes the desorption reaction easier [29]. Secondly, the presence of $Mg_2Cu$ phase apparently has catalytic effects for the hydriding and dehydriding reactions of Mg and Mg-based alloys [19]. Additionally, the addition of the third element Cu probably stabilizes the nanostructure of the alloy obtained by melt spinning, which could be very important for practical H-storage materials on the base of $Mg_2Ni$. In multicomponent Mg-based hydrogen storage alloys surface segregation and formation of microcrack passages for H-diffusion improve the kinetics of hydriding/dehydriding.

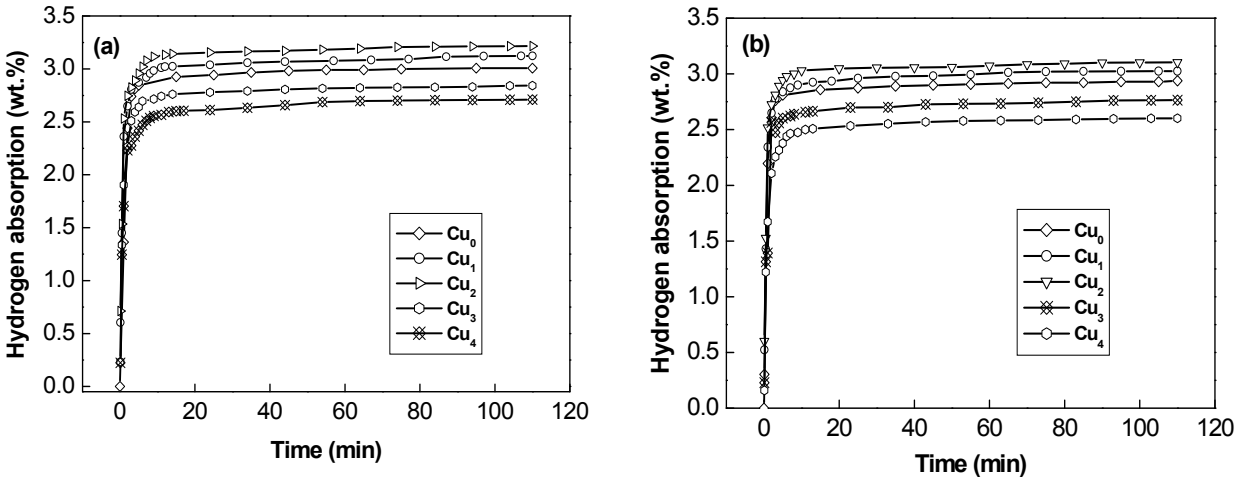


**Figure 6.** Hydrogen absorption kinetic curves of the as-spun alloys: (a) 20 m/s, (b) 30 m/s.

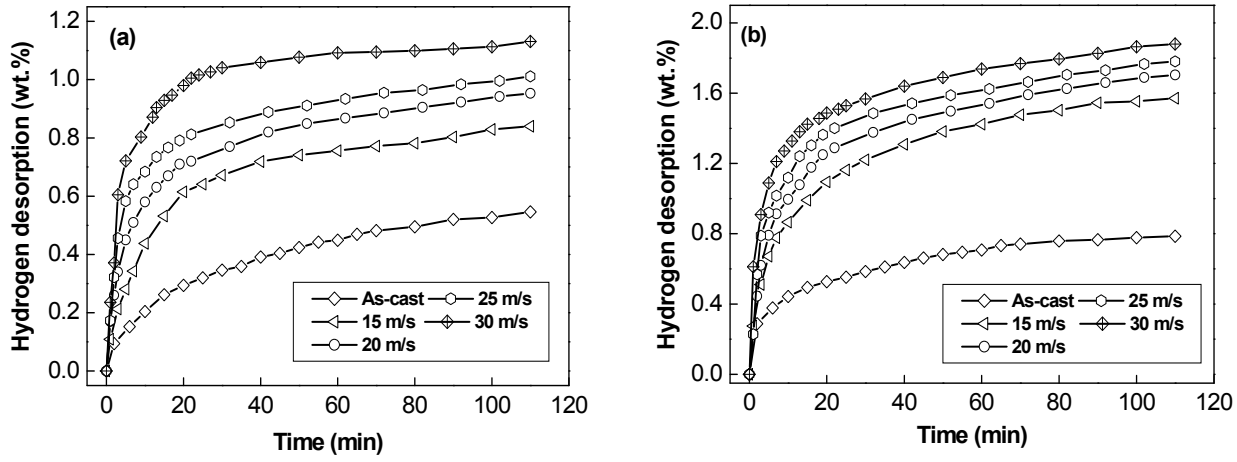


**Figure 7.** Hydrogen desorption kinetic curves of the as-cast and spun alloys: (a) $Cu_1$ alloy (b) $Cu_3$ alloy.

 

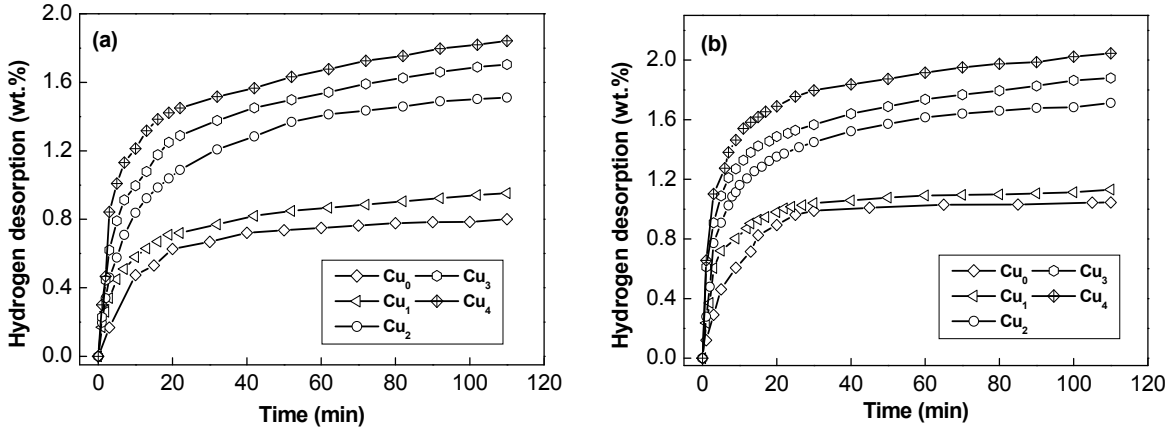


**Figure 8.** Hydrogen desorption kinetic curves of the as-spun alloys: (a) 20 m/s, (b) 30 m/s.

## 4. CONCLUSIONS

1) All the as-spun $Mg_{20}Ni_{10-x}Cu_x$ (x = 0, 1, 2, 3, 4) alloys hold nanocrystalline structures and are free of amorphous phase. The substitution of Cu for Ni does not change the major phase of the alloy, but it leads to a significant refinement of the grains and the formation of secondary phase $Mg_2Cu$ in the as-cast alloys.

2) Melt spinning significantly improves the hydriding and dehydriding properties of the alloys. Hydriding and dehydriding capacities and rates of the alloy markedly rise with increasing spinning rate, which is mainly attributed to the formation of the nanocrystalline structure caused by melt spinning.

3) With the substitution of Cu for Ni, the hydrogen absorption capacity of the alloys first increases and then decreases. But it clearly improves the hydrogen desorption capacity and dehydriding rate of the alloys, for which the decreased stability of the hydride by Cu substitution is mainly responsible.

## 5. ACKNOWLEDGEMENTS

This work is supported by Hi-Tech Research and Development Program of China (2007AA03Z227), National Natural Science Foundations of China (50871050 and 50701011), Natural Science Foundation of Inner Mongolia, China (200711020703) and Higher Education Science Research Project of Inner Mongolia, China (NJzy08071).

## REFERENCES

[1] Schlapbach, L. and Züttel, A. (2001) Hydrogen-storage materials for mobile applications [J]. *Nature*, **414**, 353-358.

[2] Simičić, M.V., Zdujić, M., Dimitrijević, R., *et al.* (2006) Hydrogen absorption and electrochemical properties of $Mg_2Ni$-type alloys synthesized by mechanical alloying [J]. *Journal of Power Sources*, **158**, 730-734.

[3] Schlapbach, L. (2002) Hydrogen as a fuel and its storage for mobility and transport [J]. *MRS Bulletin*, **27**, 675-676.

[4] Ebrahimi-Purkani, A. and Kashani-Bozorg, S.F. (2008) Nanocrystalline $Mg_2Ni$-based powders produced by high-energy ball milling and subsequent annealing [J]. *Journal of Alloys and Compounds*, **456**, 211-215.

[5] Kyoi, D., Sakai, T., Kitamura, N., *et al.* (2008) Synthesis of FCC Mg-Ta hydrides using GPa hydrogen pressure method and their hydrogen-desorption properties [J]. *Journal of Alloys and Compounds*, **463**, 306-310.

[6] Palade, P., Sartori, S., Maddalena, A., *et al.* (2006) Hydrogen storage in Mg-Ni-Fe compounds prepared by melt spinning and ball milling [J]. *Journal of Alloys and Compounds*, **415**, 170-176.

[7] Song, M.Y., Yim, C.D., Bae, J.S, *et al.* (2008) Preparation by gravity casting and hydrogen-storage properties of Mg-23.5 wt.%Ni-(5, 10 and 15 wt.%)La [J]. *Journal of Alloys and Compounds*, **463**, 143-147.

[8] Hima Kumar, L., Viswanathan, B. and Srinivasa Murthy S. (2008) Hydrogen absorption by $Mg_2Ni$ prepared by polyol reduction [J]. *Journal of Alloys and Compounds*, **461**, 72-76.

[9] Liu, X.F., Zhu, Y.F. and Li, L.Q. (2008) Structure and hydrogenation properties of nanocrystalline $Mg_2Ni$ prepared by hydriding combustion synthesis and mechanical milling [J]. *Journal of Alloys Compounds*, **455**, 197-202.

[10] Liu, F.J. and Suda, S. (1995) A method for improving the long-term storability of hydriding alloys by air water exposure [J]. *Journal of Alloys Compounds*, **231**, 742-750.

[11] Czujko, T., Varin, R.A., Chiu, C., *et al.* (2006) Investigation of the hydrogen desorption properties of Mg+10 wt.% X (X = V, Y, Zr) submicrocrystalline composites [J]. *Journal of Alloys Compounds*, **414**, 240-247.

[12] Gasiorowski, A., Iwasieczko, W., Skoryna., *et al.* (2004) Hydriding properties of nanocrystalline $Mg_{2-x}M_xNi$ alloys synthesized by mechanical alloying (M = Mn, Al) [J]. *Journal of Alloys Compounds*, **364**, 283-288.

[13] Sakintuna, B., Lamari-Darkrim, F. and Hirscher, M. (2007) Metal hydride materials for solid hydrogen storage: A review [J]. *International Journal of Hydrogen Energy*, **32**, 1121-1140.

[14] Gennari, F.C. and Esquivel, M.R. (2008) Structural characterization and hydrogen sorption properties of nanocrystalline $Mg_2Ni$ [J]. *Journal of Alloys Compounds*, **459**, 425-432.

[15] Muthukumar, P., Prakash Maiya, M., Srinivasa Murthy,

S., *et al.* (2008) Tests on mechanically alloyed $Mg_2Ni$ for hydrogen storage [J]. *Journal of Alloys Compounds*, **452**, 456-461.

[16] Recham, N., Bhat, V.V., Kandavel, M., *et al*. (2008) Reduction of hydrogen desorption temperature of ball-illed $MgH_2$ by $NbF_5$ addition [J]. *Journal of Alloys Compounds*, **464**, 377-382.

[17] Dobrovolsky, V.D., Ershova, O.G., Solonin, Yu. M., *et al.* (2008) Influence of $TiB_2$ addition upon thermal stability and decomposition temperature of the $MgH_2$ hydride of a Mg-based mechanical alloy [J]. *Journal of Alloys Compounds*, **465**, 177-182.

[18] Liang, G. (2004) Synthesis and hydrogen storage properties of Mg-based alloys [J]. *Journal of Alloys Compounds*, **370**, 123-128.

[19] Song, M.Y., Kwon, S.N., Bae, J.S., *et al.* (2008) Hydrogen-storage properties of Mg-23.5Ni-(0 and 5)Cu prepared by melt spinning and crystallization heat treatment [J]. *International Journal of Hydrogen Energy*, **33**, 1711-1718.

[20] Savyak, M., Hirnyj, S., Bauer, H.D., *et al.* (2004) Electrochemical hydrogenation of $Mg_{65}Cu_{25}Y_{10}$ metallic glass [J]. *Journal of Alloys Compounds*, **364**, 229-237.

[21] Spassov, T. and Köster, U. (1998) Thermal stability and hydriding properties of nanocrystalline melt-spun $Mg_{63}Ni_{30}Y_7$ alloy [J]. *Journal of Alloys Compounds*, **279**, 279-286.

[22] Zhang,Y.H., Li, B.W., Ren, H.P., *et al.* (2009) Hydriding and dehydriding characteristics of nanocrystalline and amorphous $Mg_{20}Ni_{10-x}Co_x$ (x=0–4) alloys prepared by melt-spinning [J]. *International Journal of Hydrogen Energy*, **34**, 2684-2691.

[23] Friedlmeier, G., Arakawa, M., Hiraia, T., *et al.* (1999) Preparation and structural, thermal and hydriding characteristics of melt-spun Mg-Ni alloys [J]. *Journal of Alloys Compounds*, **292**, 107-117.

[24] Tanaka, K., Kanda, Y., Furuhashi, M., *et al.* (1999) Improvement of hydrogen storage properties of melt-spun Mg-Ni-RE alloys by nanocrystallization [J]. *Journal of Alloys Compounds*, **293-295**, 521-525.

[25] Orimo, S. and Fujii, H. (2001) Materials science of Mg-Ni-based new hydrides [J]. *Applied Physics A*, **72**, 167-186.

[26] Mulas, G., Schiffini, L. and Cocco, G. (2004) Mechanochemical study of the hydriding properties of nanostructured $Mg_2Ni$–Ni composites [J]. *Journal of Materials Research*, **19**, 3279-3289.

[27] Zaluski, L., Zaluska, A.J. and Ström-Olsen, O. (1997) Nanocrystalline metal hydrides [J]. *Journal of Alloys Compounds*, **253-254**, 70-79.

[28] Orimo, S., Fujii, H. and Ikeda, K. (1997) Notable hydriding properties of a nanostructured composite material of the $Mg_2Ni$-H system synthesized by reactive mechanical grinding [J]. *Acta Materialia*, **45**, 331-341.

[29] Woo, J.H. and Lee, K.S. (1999) Electrode characteristics of nanostructured MgNi-type alloys prepared by mechanical alloying [J]. *Journal of The Electrochemical Society*, **146**, 819-823.